Optimizing Tricycle (Tuk-Tuk) Suspension Systems Using Mathematical Modeling

Chaiyawoot Narintharangkul[1*] and Poom Jatunitanont[2]
[1,2]Faculty of Engineering and Technology, Panyapiwat Institute of Management, Nonthaburi, Thailand
E-mail: chaiyawootnar@pim.ac.th*, poomjat@pim.ac.th

Received: February 13, 2025 / Revised: May 20, 2025 / Accepted: May 28, 2025

***Abstract*—The use of tricycles in Thailand has declined due to mechanical issues, particularly with the engine and suspension systems. This research focuses on optimizing the suspension system to improve ride comfort. The study has three main objectives: 1) to analyze the vibration of the leaf spring suspension in two-section convertible tricycles, 2) to develop a suspension model that complies with ISO 2631-1 standards for vibration comfort, and 3) to compare vibration effects between the original and new suspension models using simulation software. The goal is to reduce vibrations and enhance comfort through mathematical modeling and parameter optimization. FFT and PSD analyses identified dominant vibration frequencies in the 4 to 8 Hz range, which correspond to human body resonance. By applying a band-stop filter and optimizing spring stiffness and damping coefficient, the damping ratio was adjusted to 0.3. This led to a significant reduction in RMS acceleration from 0.985 m/s² to 0.537 m/s², and peak acceleration dropped from 1.12 m/s² to 0.582 m/s², improving comfort from fairly uncomfortable to slightly uncomfortable.**

The optimized suspension design significantly reduced vibrations in critical frequency ranges. The results from this approach can be applied to various vehicle types, offering potential for further development in the automotive industry, especially for vehicles sensitive to vibration.

***Index Terms*—Tricycle, Suspension System, Vibration, Comfort Value, Computer Program**

I. Introduction

The Tuk-Tuk, officially known as the Tricycle, was first produced in 1948 by Piaggio Ape, an Italian company also known for manufacturing Vespa. The tricycle produced at that time had a top speed of 30 miles per hour. Since then, the Tuk-Tuk has been introduced and gained popularity in many countries across Asia. It was first manufactured in Asia in 1957 when Japan began selling three-wheeled trucks.

The Daihatsu Midget DK is a two-stroke motorcycle (ZA 250cc) with a single headlight and motorcycle-like handling. Shortly thereafter, this tricycle model was imported to Thailand for the first time in 1960 to replace pedal tricycles that were banned in Bangkok. Initially, the Japanese tricycles were modified with a roof for passenger safety and to close the access on the right side. Originally, there were two access points for passengers, but later, this was changed to only one for safety reasons.

Initially, there were many brands of tricycles, but today, only a few remain. Thus, the tricycle has been a long-standing symbol of Thailand. According to the Automobile Act No. 18, 2019, tricycles can be divided into two types: personal tricycles (Ror-Yor. 4) and three-wheeled taxis (Ror-Yor. 8). A survey conducted as of July 31, 2022, found that there was a total of 20,207 three-wheeled vehicles in use across the country, including both personal tricycles and three-wheeled taxis, which is fewer than the 20,484 vehicles registered as of December 31, 2021. This decrease is attributed to the non-approval of vehicle registration due to failing inspection according to the Department of Land Transport's regulations [1].

Inside the tricycle, there are systems similar to those found in general cars, which can be divided into six categories: engine system, transmission system, steering system, braking system, electrical system, and suspension system. Currently, tricycle owners in Thailand focus on enhancing engine performance to increase speed and power. However, this focus may impact the engine's lifespan and contribute to air pollution due to black smoke from increased engine performance. Comparative studies between Thai and foreign tricycles reveal that tricycles abroad emphasize passenger comfort, focusing more on the suspension system than on other systems. The main function of the suspension system is to dampen vibrations between the road surface and the vehicle to improve road grip. If the suspension is inadequate, hitting a bump can disrupt the vehicle's balance and potentially affect passengers.

The suspension system of Thai tricycles is designed with a rigid beam and leaf springs, which

have both advantages and disadvantages. This system often faces problems, such as excessive weight under the springs, which affects vehicle control at high speeds and on rough roads. Without proper maintenance and with overloading, the leaf spring suspension is more suitable for carrying goods than passengers. This is because the force from the suspension is directly transmitted to the vehicle frame, causing passengers to feel the impact as well.

In today's rapidly advancing automotive world, every system in all types of vehicles is continuously evolving. Changes in engine systems, from internal combustion engines to electric engines, and improvements in suspension systems are significant. Analyzing and developing components or creating new ones to enhance user or passenger comfort and driving smoothness is crucial. This aligns with research by Jaisaard, research conducted a comparative study of ride quality between the EMU-A1 and EMU-B1 trains on the BTS Sukhumvit Line from stations N8 to E14. Although the study encompasses various measurements, testing was not conducted on different types of road surfaces.

This study investigates the design, analysis, and improvement of the suspension system for Thai tricycles to enhance ride comfort, vibration isolation, and load-bearing capacity. Using mathematical modeling and simulation, the research provides a robust framework for evaluating suspension performance. The findings support the development of Thai tricycles to meet international standards and competitiveness. Moreover, the insights gained apply to a wide range of vehicles such as motorcycles, trucks, and buses, offering potential benefits in both commercial and industrial applications through improved damping and vibration control.

A. Objectives of Research

- Research and analyze the vibrations of the leaf spring suspension in two-section convertible tricycles currently in use.
- To develop a model that complies with the ISO 2361-1 standard, the design and layout of the new tricycle suspension ensure standard vibration comfort.
- To compare the vibration effect of the model of the old and new undercarriage parts of the tricycle that received vibration through a computer program.

B. Research Hypothesis

- Tricycles are used by Thai citizens and international visitors in daily life for travel or transportation.
- Passenger comfort in riding in a tricycle with the original suspension is less comfortable than the new suspension.
- The vibration of the new suspension can be used better in traffic.

C. Scope of Research

- This study investigated the vibration of the plate spring suspension of the current model tricycle. This is a two-stage convertible tricycle.
- Study by modeling old and new tricycle suspensions in various ways to analyze the vibration of the suspension of tricycles currently in use according to ISO 2361-1.
- Analyze the suspension model of the currently in-use convertible tricycle in 1D and compare the effect of vibration using a computer program.

D. Benefits

- Increase the efficiency of the suspension system of the tricycle to absorb vibration better than before
- The improved suspension design can be applied to other forms of tricycles.
- Can promote and attract the use of tricycles.
- Can be used to extend the business of tricycles.

E. Definition

- Tricycle means a Tuk-Tuk or a tricycle that is hired to carry passengers with a two-part convertible.
- The suspension system refers to the components of the vehicle below all. Which is the part that supports the entire weight of the car?
- Simulation software is used to solve and analyze the data.

II. Literature Review

A. Suspension

A vehicle's suspension system is designed to absorb and minimize vibrations generated by contact with the road surface. Positioned between the car's frame, body, engine, transmission, and wheels, the suspension ensures that road irregularities do not disrupt the vehicle's smooth operation. Its primary function is to dampen the impact of vibrations from tire-road interactions, preventing excessive transmission of these vibrations into the cabin. Beyond this, the suspension system plays a crucial role in maintaining the vehicle's stability, ensuring proper body alignment, and keeping the tire tread perpendicular to the road surface, even during turns. It also helps to control excessive bouncing, reduce unwanted movements, and maintain balance, particularly when navigating uneven terrain or during rapid acceleration and braking [2].

B. Vibration

The vibration of an object relies on Newton's law of motion, as shown in (1) (Newton's law of motion), to find the differential equation of motion.

$$\sum F = m\vec{\ddot{x}}(t) \quad (1)$$

Newton's second law equation is that the sum of the applied force $\sum \vec{F}(t)$ is equal to the mass m times the acceleration, where the variable x(t) is the vibrational distance $\dot{x}(t)$. The vibration velocity, and x(t) is the acceleration of the vibration, which are variables that can change over time. Therefore, the value of the vibration distance that occurs in the system will be a value that can change over time when an external force acts. The vibration problem consists of three main components: the spring constant. The weight of the mass and the damping constant by the spring constant are used to store the potential energy of the system. The force generated by the extension or contraction of the spring can be calculated from (2) [3].

$$F_k = kx(t) \quad (2)$$

Where k is the spring constant in N⁄m and x(t) is the extension of the spring in meters, which is a time-varying value by which the force of the spring is used to pull or push the mass back. Ideally, if the system does not have a device for extracting the energy of the vibration, the mass of the system will vibrate without stopping, so the final component of the A damper is a damper that is used to extract the potential energy from the spring from the system to stop the vibration. The force generated by the damper device can be shown as (3).

$$F_c = c\dot{x}(t) \quad (3)$$

Where c is the damper constant in and $\dot{x}(t)$ is the mass vibration velocity in m/s. Used to reduce vibrations that occur in the system [4].

The vehicle suspension system, as shown in Fig. 1, is an illustration of the suspension system of one side of a wheel, which has all 3 vibration components. In mathematical modeling, the mass of the vehicle frame is given by the variable $m_{s,}$ and the mass of the car wheels with tires is given by the variable m_u, which is in kg. The mass of the vehicle frame accounts for only one quarter of the total vehicle weight, as represented in the Quarter Car model. Spring component is used to simulate the elasticity of a spring at suspension, which is defined as k_s variable and used to simulate the elasticity of a tire, which uses the k_u variable to simulate the tire section, and the c_s variable is used to simulate the damper. That is in the lower area, in which to create a mathematical model, a diagram of the forces occurring in the system must be drawn (free-body diagram), where the variable x (t) is the vibration distance in the vertical mass of the vehicle frame. The variable y (t) is the vertical vibration distance of the vehicle wheels, and the variable z(t) is the level of the road the vehicle travels on. These three variables are time-varying. Forces arising in the spring and damping elements between the vibration stages x(t) and y(t) or y(t) and z(t) are due to the difference in the vibration stages of the masses. The frame and wheel mass for the spring force and the resulting difference in the velocity of the vibration of the frame and wheel mass for the damper element, respectively.

In the simulation, the car will run on a flat road or value *z(t) = 0* where z is the road level used to simulate the car on a flat road, and the value *z(t) > 0* represents the car driving on different roads. As a result, vibrations are generated at the mass of the car frame and wheels, with the suspension comprising spring elements and dampers working together to reduce the level of vibration, as shown in Fig. 1 [5].

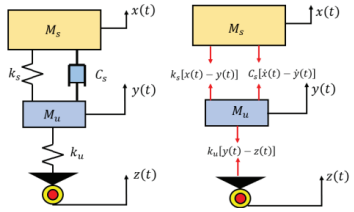

Fig. 1. Mathematical modeling of automotive suspension systems

To find a mathematical model, it relies on Newton's second law to find the equation of motion by analyzing the mass of the car frame, m_s, and the mass of the car wheel m_u, which can be calculated. The motion in terms of second-order differential equations (4) and (5) is obtained respectively from Newton's second law, which determines the direction of vibration of the mass of the frame m_s. And the mass of the wheel m_u is positive when both masses are moving upward.

$$\ddot{x} = -[(k_s/M_s)x(t)]+[(k_s/M_s)y(t)] - [(C_s/M_s)\dot{x}(t)]+[(C_s/M_s)\dot{y}(t)] \quad (4)$$

$$\ddot{y}(t) = [(k_s/M_u)x(t)]-[(k_s/M_u)y(t)]+ [(C_s/M_u)\dot{x}(t)]-[(C_s/M_u)\dot{y}(t)]- [(k_u/M_u)y(t)]+[(k_u/M_u)z(t)] \quad (5)$$

Equations (4) and (5) can be written in state-space form as (6).

$$\dot{\vec{x}}(t) = [A]\vec{x}(t)+[B]\vec{u}(t) \quad (6)$$

Where $\dot{\vec{x}}(t)$ is the velocity vector, $\dot{\vec{x}}(t)$ is the position vector, and the variable $\vec{u}(t)$ is the incoming signal vector or road level z(t), where the matrix [A] is the system matrix and matrix [B] is the input matrix, since the left side of (6) is the order derivative velocity vector. Therefore, to write (4) and (5) in terms of first derivatives as shown in (6), one of the variables to reduce the power of the derivative from second order to first order by setting the variable as shown in (7).

$$x_1(t) = x(t) \quad (7)$$

Equation (7), the variable from is the vibration distance of the vehicle frame. x(t), then defines the

variable , as shown in (8).

$$x_2(t) = \dot{x}_1(t) = \dot{x}(t) \quad (8)$$

From (8), the variable $x_2(t)$ is the vibration velocity of the car frame $\dot{x}(t)$, so $\dot{x}_2(t)$ is equal to $\ddot{x}(t)$ or the acceleration of the car frame. Set the variable $x_3(t)$ as shown in (9) and the variable $x_4(t)$ to be the first derivative of the variable $x_3(t)$ as shown in (10).

$$x_3(t) = y(t) \quad (9)$$

$$x_4(t) = \dot{x}_3(t) = \dot{y}(t) \quad (10)$$

From defining variables, it can be found that $x_3(t)$ is the vibration distance of the car wheels, and the variable $x_4(t)$ is the speed of the vibration of the car wheels. Therefore, if using the variable $x_4(t)$ to get the first derivative, Equation (11), which is equal to the acceleration of the wheels of the car.

$$\dot{x}_4(t) = \ddot{x}_3(t) = \ddot{y}(t) \quad (11)$$

By defining a new variable to reduce the order of the differential equations, (4) and (5) can be written in terms of spatial equations as shown in (6). Equation (6) is rewritten in the form of (12).

$$\begin{bmatrix} \dot{x}_1(t) \\ \dot{x}_2(t) \\ \dot{x}_3(t) \\ \dot{x}_4(t) \end{bmatrix} = \begin{bmatrix} 0 & 1 & 0 & 0 \\ -k_s/M_s & -C_s/M_s & k_s/M_s & C_s/M_s \\ 0 & 0 & 0 & 1 \\ k_s/M_u & C_s/M_u & -\left(\frac{k_s}{M_u}+\frac{k_u}{M_u}\right) & -C_s/M_u \end{bmatrix} \begin{bmatrix} x_1(t) \\ x_2(t) \\ x_3(t) \\ x_4(t) \end{bmatrix} + \begin{bmatrix} 0 \\ 0 \\ 0 \\ k_u/M_u \end{bmatrix} z(t) \quad (12)$$

when the variable

$x_1(t)$ is the vibration distance of the chassis in m.

$x_2(t)$ is the vibration velocity of the chassis in m/s.

$x_3(t)$ is the vibration distance of the wheel in m.

$x_4(t)$ is the speed of vibration of the wheels in m/s.

The spatial equation of state (12) will be used to simulate the vibration effects occurring in the vehicle suspension system as the vehicle travels across different surfaces, using the variables in matrices [A] and [B]. These variables will remain constant throughout the vibrations occurring in the car suspension system.

C. Assessment of Driving Comfort According to ISO 2631-1

Humans respond at different frequencies. Therefore, the ISO 2631-1 standard has a different value of the weighting factor at each frequency. The scope of content in ISO 2631-1 indicates methods for measuring the different types of visual vibrations entering human subjects. Whether sitting, standing, or lying down, this is found in driving vehicles. Mechanization or in a residential area, and tell them to calculate the indicator, indicating the level of vibration that can be tolerated. In terms of health, comfort, perception, or nausea, humans could perceive each frequency differently. Therefore, there is a weight to be calculated for each frequency as well. This value is called frequency weightings, which consists of W_k, W_d, W_f, W_c, W_e, W_j, which are used depending on the axis of the vibration according to ISO 2631-1, which is used to assess the acceleration of the passenger. In a sitting position, in case the force is exerted from under the seat, for example, the relationship between the weighting factor *(W)* and the frequency in the case of a passenger's sitting position will be used to weigh the acceleration of the support spring mass after converting to a signal in the frequency domain [6]. The effectiveness of the total acceleration can be expressed as the following equation.

$$A_w = [\sum (W_i A_i)^2]^{1/2}$$

The total effective acceleration values can be used to assess driving comfort according to the recommended criteria as follows.

1. When less than 0.315 m/s^2 is not an uncomfortable level.
2. When between 0.315 m/s^2 - 0.63 m/s^2, it feels a bit uncomfortable.
3. When between 0.5 m/s^2 - 1 m/s^2, it feels fairly uncomfortable.
4. When between 0.8 m/s^2 - 1.6 m/s^2, it feels uncomfortable.
5. When between 1.25 m/s^2 - 2.5 m/s^2, it feels very uncomfortable.
6. When more than 2 m/s^2 is at an extremely uncomfortable level.

D. Vibration Measuring Device

- Arduino Board

Arduino is a small AVR microcontroller board that serves as a processor and controller, making this device ideal for studying and learning about microcontroller systems. The board can control a wide range of input/output devices, either independently or in conjunction with other devices, such as PCs. This is possible because Arduino supports connection to various digital and analog input/output devices, including receiving data from switches or sensors and controlling output devices like LEDs, motors, relays, and more. An Arduino hardware system can be created and assembled by the user, who should have some basic knowledge of electronics, or pre-made circuit boards can be purchased, available at affordable prices [7].

- Vibration Sensor

A vibration sensor is an instrument designed to measure the magnitude and frequency of vibrations within a system, machine, or piece of equipment. These measurements are utilized to identify imbalances or other potential issues within the asset, aiding in the prediction of future failures. A vibration sensor can be directly connected to the asset or monitored wirelessly. Once installed, the sensor detects vibrations from the

asset through various methods, depending on the type of sensor employed. Over time, the device generates two types of data: frequency and intensity [8].

In the research, the basic system variables will be determined. Variable values can be determined as shown in Table I. The values of the variables are based on research of Ceyhanli [9] for being the default variable value in simulating the vibration of the car suspension. The characteristics of the leaf spring car suspension determine the durability and stretch of the leaf springs.

TABLE I
VALUES OF THE TRICYCLE SUSPENSION MODEL

Variable	Result	Unit
k_1	479.92	N/m
k_2	509.6	N/m
J_0	140.073	Kg-m^2
d_1	0.64	m
d_2	0.64	m
M	350	kg

The K value of the spring (Spring Rate) is the softness of the spring that will collapse in proportion to the weight of the vehicle pressed down onto the spring coil. The value has been measured using a measuring tool to find out the value. The tool used is a spring stiffness meter. The values that can be measured are k_1 = 479.92 N/m and k_2 = 509.6 N/m, as mentioned in the table above.

Fig. 2. Shock Spring hardness measuring tool

The Shock Spring Hardness Measuring Tool is specialized equipment engineered and manufactured in accordance with national standards for spring tension and compression testing machines. It is designed for testing various properties of springs, including tensile strength, pressure, displacement, deformation, hardness, and free height. In the context of experimental methodology, research experiments are conducted using a system of mathematical equations to derive the results. The experimental process is divided into three distinct phases by the researcher.

III. METHODOLOGY

A. Mathematical Calculation

The researcher has developed a Free Body Diagram (FBD) illustrating the forces acting on the suspension system of the tricycle, comprehensively depicting all the forces involved. This diagram was then compared with the tricycle used as a sample in the study. Furthermore, the researcher employed an engineering drawing program to create a detailed design, thereby enhancing the visualization of the three-wheeled suspension system's components. This method also contributes to a more precise and clearer understanding of the operational principles of the suspension system.

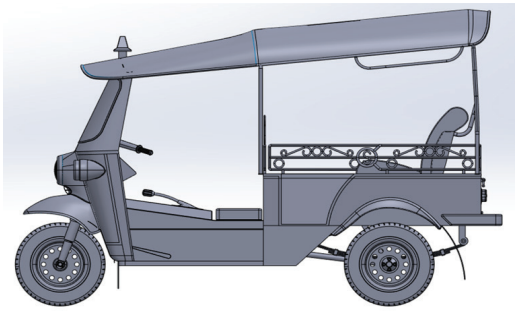

Fig. 3. Model of a tricycle through an engineering drawing program

Free Body Diagram of a tricycle can be categorized into two types: one depicting the tricycle's vibration up and down, and another representing the tricycle's motion while turning right or left. The researcher identified a problem during turning and focused on developing a free-body diagram for the tricycle while it was turning. This scenario can also be compared to the effect of a vehicle falling into a hole.

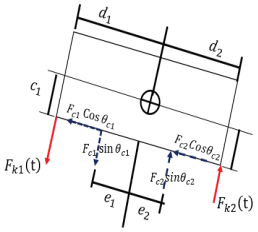

Fig. 4. Free-body diagram occurs while the tricycle makes a turn.

The equations of motion of a two-degree-of-freedom (Equation of Motion) system can be written as a system of equations using knowledge of algebra. Matrices and vectors can help with writing equations as follows [10].

$$[m]\ddot{\vec{x}}(t)+[c]\dot{\vec{x}}(t)+[k]\vec{x}(t)=\vec{F}(t) \quad (13)$$

Therefore, the final matrix equation used to calculate this mathematical equation of the tricycle will be as follows.

$$\begin{pmatrix} -m\omega^2+k_1+k_2 & -k_1d_1+k_2d_2 \\ -k_1d_1+k_2d_2 & -J_0\omega^2+k_1d_1^2+k_2d_2^2 \end{pmatrix} \begin{Bmatrix} X \\ \Theta \end{Bmatrix} = \begin{Bmatrix} 0 \\ 0 \end{Bmatrix} \quad (14)$$

By the method of finding the value of the matrix equation after substituting the values X and $\Theta \neq 0$, the equation can be found using the Determinant method. This method is a function that gives the result as a scalar quantity. Which depends on the value of n in the n×n dimension of the square matrix. From the Determinant method, the equation will be obtained ω^4 and ω^2 in the form of an equation with the values of and in the equation. Arrange the form ω^2 of the equation so that, in the form ω^2 of the equation, both the equation and when reformatting it stay in the equation. The entire equation must then be assigned the variable $\lambda=\omega^2$ to the equation, and the roots of the equation that has been specified can be found. Obtained by using the Quadratic Formula equation.

$$a\lambda^2+b\lambda+c=0 \rightarrow -b\pm\sqrt{b^2+4ac}/2a \quad (15)$$

After knowing the values of ω_1 and ω_2, find the values of $X^{(1)}$ and $\Theta^{(1)}$ by substituting ω_1 into the equation and find the values of $X^{(2)}$ and $\Theta^{(2)}$ by substituting ω_2 into the equation as well. When the results of the variable values are obtained, determine the ratio of the maximum amplitudes of ω_1 and ω_2 as follows

$$r_1 = \Theta^{(1)} / X^{(1)} \quad (16)$$

$$r_2 = \Theta^{(2)} / X^{(2)} \quad (17)$$

After that, solve the equation using the Mode Shapes Vector principle to find the values $\vec{x}^{(1)}$ and $\vec{x}^{(2)}$ by substituting the values in the equation from the values r_1 and r_2 using the following equation.

$$\vec{X}^{(1)} = \begin{Bmatrix} 1 \\ r_1 \end{Bmatrix} X^{(1)} \quad (18)$$

$$\vec{X}^{(2)} = \begin{Bmatrix} 1 \\ r_2 \end{Bmatrix} X^{(2)} \quad (19)$$

Therefore, to substitute the equation to find a vibration diagram of the suspension system, it must occur at a certain time. The equation used must, therefore, be as follows.

$$\vec{X}^{(1)}(t) = \begin{Bmatrix} X^{(1)}(t) \\ \theta^{(1)}(t) \end{Bmatrix} = \begin{Bmatrix} 1 \\ r_1 \end{Bmatrix} X^{(1)} \cos(\omega_1 t+\emptyset_1) \quad (20)$$

$$\vec{X}^{(2)}(t) = \begin{Bmatrix} X^{(2)}(t) \\ \theta^{(2)}(t) \end{Bmatrix} = \begin{Bmatrix} 1 \\ r_2 \end{Bmatrix} X^{(2)} \cos(\omega_2 t+\emptyset_2) \quad (21)$$

Equations (20) and (21) mentioned above are First Mode and Second Mode equations, respectively, as mentioned above. After that, substitute the obtained equation with the solution equation into (3) [11]. The solution equation can be written as

$$X_1(t) = X_1 \cos(\omega t+\emptyset) \quad (22)$$

$$\dot{X}_1(t) = -X_1 \sin(\omega t+\emptyset)d/dt(\omega t+\emptyset) \quad (23)$$

$$\ddot{X}_1(t) = -X_1 \omega\cos(\omega t+\emptyset)d/dt(\omega t+\emptyset) \quad (24)$$

$$X_2(t) = X_2 \cos(\omega t+\emptyset) \quad (25)$$

$$\dot{X}_2(t) = -X_2 \sin(\omega t+\emptyset)d/dt(\omega t+\emptyset) \quad (26)$$

$$\ddot{X}_2(t) = -X_2 \omega\cos(\omega t+\emptyset)d/dt(\omega t+\emptyset) \quad (27)$$

When the solution equation has been successfully substituted into variables $X(t)$, $\dot{X}(t)$ and $\ddot{X}(t)$ in the mathematical model. The solution of the equation will be found in (22) and (25), also be found that in term $\cos(\omega t+\emptyset)$, it cannot be equal to 0 because it will not be possible to find the solution of the equation, and from (22) and (25), must be arranged in the form of a matrix equation. to proceed to the next step. After getting the matrix equation, the variables X_1 and X_2 will be found, that is, X_1 will have a value equal to the Maximum amplitudes of $X_1(t)$ and $X_2(t)$ it cannot be equal to zero because if it is equal to 0, it indicates no vibration, which is not possible. The next step will be to use the Modal principle to find the values $X_1^{(1)}$ and $X_1^{(2)}$ by finding those values with the following equation.

$$\vec{X}(0) = [X]^t[M]\vec{X}(0) \quad (28)$$

In the final step, the natural frequency (Natural Frequency) or values 1 and 2 have been obtained by solving the equations mentioned above, including the values 3 and 4 from calculations through the Modal principle from Mode Shape. Vector, therefore, can be used to find the value of the Modal Matrix by finding from the equation as follows

$$[X] = [\vec{X}^{(1)} \quad \vec{X}^{(2)}] \quad (29)$$

When the value [X] is obtained at a certain time, it must find the coordinates q by assigning it 180° = πrad. To find the coordinates, use the equation to find the coordinates as follows.

$$\vec{q}(0) = [X]^t[M]\vec{X}(0) \quad (30)$$

Use the solution equation of the method to find coordinates when i=1 and i=2, then the solution equation will be used as follows.

$$q_i(t) = q_i(0) \cos \omega_i t + (q_i(0)/\omega_i)\sin \omega_i t \quad (31)$$

When solving the equation, the values $q_i(t) = q_i(0) \cos \omega_i t$ and $q_i(t)$ will be obtained as follows.

$$q_1(t) = q_1(0) \cos \omega_1 t \quad (32)$$

$$q_2(t) = q_2(0) \cos \omega_2 t \quad (33)$$

When the value q is obtained, it will be put into the equation to find the value $\vec{X}(t)$ by specifying the equation for finding the value as follows.

$$\vec{X}(t) = [X]\vec{q}(t) \quad (34)$$

B. Transfer function matrix: Two degrees of freedom suspension model

A transfer function matrix is a fundamental concept in control systems and systems engineering, especially when dealing with Multiple-Input Multiple-Output (MIMO) systems. It extends the idea of a single transfer function, which relates one input to one output, to systems with multiple inputs and outputs. This matrix-based approach allows for the analysis and design of complex systems where multiple variables interact simultaneously. The details of this method are explained in the following section [12].

- Transfer function model of suspension system

For a tricycle vehicle suspension system modeled as a 2 Degrees of Freedom (DOF) mass-spring-damper system, the system consists of the sprung mass (vehicle body) and the unsprung mass (wheel assembly). The inputs to the system are typically road profiles, which can be considered as external forces or displacements applied to the system. Consider Fig. 6 for a vehicle suspension system. When m_s is sprung mass or vehicle body mass, m_u is unsprung mass or wheel assembly mass, k_s is spring constant of the suspension spring, k_t is spring constant of the tire, C_s is damping coefficient of the suspension damper, $x_s(t)$ is displacement of the sprung mass from its equilibrium position, $x_u(t)$ is displacement of the unsprung mass from its equilibrium position and r(t) is road profile input or displacement of the road.

The transfer function matrix G(s) encapsulates the dynamic relationship between the road profile input R(s) and the displacements $X_u(s)$ and $X_s(s)$ of the unsprung and sprung masses, respectively, in the 2 DOF mass-spring-damper system of the vehicle. This transfer function is crucial for analyzing the response of the vehicle suspension system to road disturbances and for designing system parameter values to improve ride comfort and handling.

$$G(s)=\frac{X_s(s)}{R(s)}=\frac{k_t}{(m_s s^2+C_s s+k_s)(m_u s^2+C_s s+k_s+k_t)-(C_s s+k_s)^2} \quad (35)$$

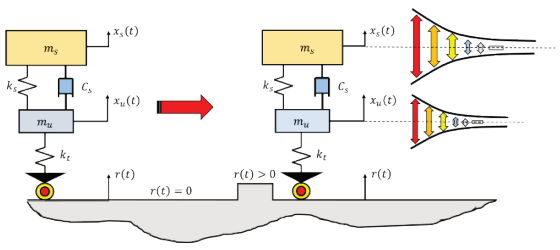

Fig. 5. A vehicle suspension system

- The system parameters of the transfer function model in the suspension system

The system parameters, such as, k_s, is spring constant of the suspension spring, k_t the spring constant of the tire, C_s is damping coefficient of the suspension damper have been measured by shock and spring measurement tool as shown in Fig. 6. The spring constant of two leaf springs and the damping coefficient of two shock absorbers are determined using a shock and spring measurement tool. Load cell sensors are used to measure the applied force from an external source. The value of applied force and displacement of the leaf spring from the origin are used to determine the spring constant value. The damping coefficient is determined by using the applied force and the rate of displacement. The transfer function matrix G(s) is used to draw the Bode plot, which is a graphical representation that shows how the system responds to different frequencies of road disturbance input. The Bode plot is a powerful tool for understanding how the suspension responds to road disturbances at different frequencies. It helps in designing and tuning the suspension to improve ride comfort and vehicle handling.

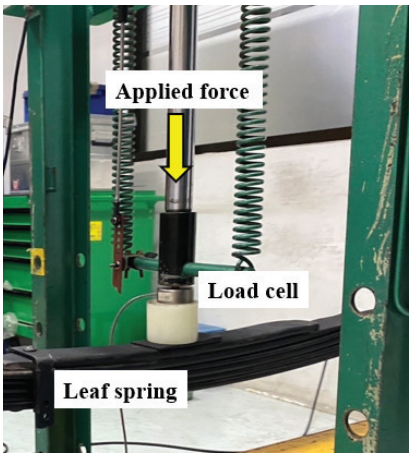

Fig. 6. A shock and spring measurement tool

C. Natural Frequency of the Vehicle Suspension System

The natural frequency of a two-degree-of-freedom (2DOF) vehicle suspension system refers to the frequency at which each mass (sprung and unsprung) tends to oscillate when not subjected to any external force (e.g., road input or damping). These frequencies are crucial in the design of vehicle suspension systems as they directly affect ride comfort and handling. The steps to find the natural frequencies are explained in the following section.

- Solve the characteristic equation

The natural frequencies are found by solving the characteristic equation derived from the determinant of the matrix equation of free vibration of the vehicle suspension system.

$$\det([K]-\omega^2[M])=0 \quad (36)$$

Where ω is the natural frequency? The determinant of the characteristic equation is used to determine ω^2 in the polynomial equation. The roots of ω^2 are ω_1, and when ω_1 and ω_2 are the natural

frequencies of vehicle body mass and wheel mass, respectively. The natural frequencies of a vehicle suspension system are essential parameters in vehicle dynamics, affecting both ride comfort and vehicle handling. These frequencies can be determined by modeling the system with equations of motion, forming the mass and stiffness matrices, solving the characteristic equation, and then computing the frequencies from the eigenvalues obtained [13].

- Vibration Data Collection

Two MPU-6050 sensors were utilized to measure the acceleration of a vehicle's body mass and two-wheel masses, respectively. The wiring diagram for the two MPU-6050 sensors is shown on Fig. 7. To measure the vibration data, an Arduino UNO connected to a 5 VDC power supply, two MPU-6050 sensors, and an HC-05 Bluetooth module were used to record the experimental data. The Bluetooth module sent the measured data signal to the computer via Bluetooth signal. The first MPU-6050 sensor was attracted to passenger seat of tricycle for measuring the acceleration of a vehicle's body mass and the second MPU-6050 sensor was attracted at differential gear for measuring the acceleration of wheel mass as shown in Fig. 7. The responds of the displacement at a vehicle's body mass and wheel mass have been used to identify two natural frequencies mode by the Fast Fourier transform method. When the tricycle was operated at a speed of 40 km per hour for the duration of 1,200 seconds in a straight line. Some limitations of this experiment include the potential drift and noise of MPU-6050 sensors, limited sampling rate, and possible data loss during Bluetooth transmission and environmental effects such as temperature and vibration. Additionally, the sensor placement may not perfectly represent the actual mass centers, and motion was assumed to occur mainly in one direction without cross-axis compensation.

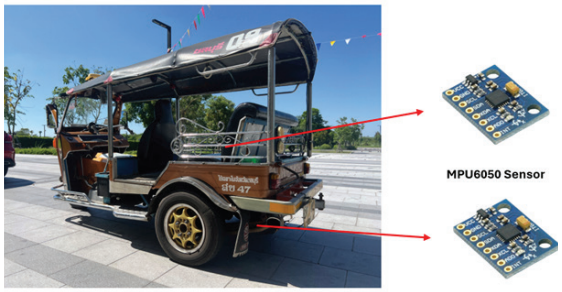

Fig. 7. The location of two MPU-6050 sensors in tricycle vehicles

- Determine natural frequency using the Fast Fourier Transform

Before performing calculations through the program, a real experiment must first be conducted to obtain experimental values. These values are used to verify that the calculated values, derived from the formulas, do not deviate by more than 10% from the values obtained through the actual experiment with the tricycle used as the test subject. This experiment was carried out using a two-section convertible three-wheeled vehicle. The tricycle was tested at three different speed ranges: 20, 30, and 40 kilometers per hour (km/h). The distance used for each test lap was 700 meters, with a total of two test runs conducted at each speed, equivalent to one test lap. Thus, each test run covered a distance of 1.4 kilometers (1,400 meters). The route used in the test will be the route of the road within the Panyapiwat Institute of Management, EEC Campus. The route will include 4 left curves, 1 right curve, and 3 uphill turns. Another method to determine the natural frequency is to measure the time-domain response of the vehicle suspension system using accelerometer sensors. The data should capture the displacement, velocity, or acceleration of the sprung and unsprung masses over time. This data is typically collected after the system is subjected to an impulse or step input, which excites the system's natural frequencies. The Fast Fourier transform is a computational algorithm used to convert the time-domain signal into the frequency domain. It will give you a spectrum showing the amplitude or power of each frequency component present in your signal. The Fast Fourier Transform is an efficient algorithm to compute the Discrete Fourier Transform of a sequence. The DFT converts a finite sequence of equally spaced samples of a function in the time domain into a sequence of coefficients of a finite combination of complex sinusoids [14]. The DFT equation can be shown as

$$X[k]=\sum_{n=0}^{N-1} x[n]\cdot e^{-j\cdot 2\pi\cdot k\cdot n/N}$$

$$\text{for } k=0,1,2,\cdots, N-1 \qquad (37)$$

Where X[k] is the DFT coefficient for the frequency component, x[n] is the input sequence in time-domain data, is the total number of samples, and the term $e^{-j\cdot 2\pi\cdot k\cdot n/N}$ is the complex exponential representing the frequency component. The natural frequencies correspond to the peaks in the FFT spectrum. The peaks can be identified from the plot of the DFT. Typically, the first peak corresponds to the natural frequency of the sprung mass, and the second significant peak corresponds to the unsprung mass.

D. Comparison with Driving Comfort Standard According to ISO 2631-1

The content area of ISO 2631-1 describes methods for measuring vibrations in various images entering the human body. Whether it's the posture of sitting, standing, or lying down, which is found in driving vehicles. Use of machinery or living in a residence, and the calculation of indicators indicating acceptable levels of vibration. In terms of health, Comfort, and awareness are the main ones.

The total effective acceleration value obtained can be used to evaluate driving comfort according to the recommended criteria as follows.

1. When less than 0.315 m/s^2 is not an uncomfortable level.
2. When between 0.315 m/s^2 - 0.63 m/s^2, it feels a bit uncomfortable.
3. When between 0.5 m/s^2 - 1 m/s^2, it feels fairly uncomfortable.
4. When between 0.8 m/s^2 - 1.6 m/s^2, it feels uncomfortable.
5. When between 1.25 m/s^2 - 2.5 m/s^2, it feels very uncomfortable.
6. When more than 2 m/s^2 is at an extremely uncomfortable level.

E. Optimum System Parameter Values with Driving Comfort Standard

From mathematical models, the simulation results of vehicle vibration in various system parameter values are used to set up a function of system parameter values due to the maximum acceleration of the vehicle's body mass and wheel mass. The variations of system parameter values in simulation results are set to ± 10% and ± 20% from the tested spring and damper values. Therefore, the function of maximum acceleration of the vehicle' body mass and wheel mass can be written as a polynomial model [15].

$$f(k_s, C_s)=a_1k_s^2+a_2C_s^2+a_3k_sC_s+b \quad (38)$$

The polynomial equation can be expanded into matrix form as

$$\underbrace{\begin{matrix} f(k_{s1}, C_{s1}) \\ f(k_{s2}, C_{s2}) \\ f(k_{s3}, C_{s3}) \\ \vdots \\ f(k_{sN}, C_{sN}) \end{matrix}}_{Y} = \underbrace{\begin{bmatrix} k_{s1}^2 & C_{s1}^2 & k_{s1}C_{s1} & 1 \\ k_{s2}^2 & C_{s2}^2 & k_{s2}C_{s2} & 1 \\ k_{s3}^2 & C_{s3}^2 & k_{s3}C_{s3} & 1 \\ \vdots & \vdots & \vdots & 1 \\ k_{sN}^2 & C_{sN}^2 & k_{sN}C_{sN} & 1 \end{bmatrix}}_{X} \underbrace{\begin{bmatrix} a_1 \\ a_2 \\ a_3 \\ b \end{bmatrix}}_{\beta} \quad (39)$$

The minimum values of k_s and C_s result in simpler manufacturing processes due to fewer leaf spring plates and reduced density in the damper. The minimum values of k_s and C_s must still ensure that the vibration of the vehicle's body mass and wheel mass meets the driving comfort standards. The critical values of k_s and C_s can be determined by the first derivative of the function representing maximum displacement as.

$$\partial f(k_s, C_s)/\partial k_s=0 \quad (40)$$

$$\partial f(k_s, C_s)/\partial C_s=0 \quad (41)$$

To check the minimum fixed points, the second derivative of the functions is certainly positive, which is enough to guarantee minimum fixed points.

$$\partial^2 f(k_s, C_s)/\partial k_s^2>0 \quad (42)$$

$$\partial^2 f(k_s, C_s)/\partial c_s^2>0 \quad (43)$$

From the polynomial equation, the equation can be rewritten as a regression equation.

$$Y = X\beta+ \varepsilon \quad (44)$$

ε is the error between the measurement signal and the model output from the polynomial equation. For the identification of β column vector, the least square method has been used by summing of squares of error.

$$SSE=(Y-X\beta)T(Y-X\beta) \quad (45)$$

Taking the partial derivative of with parameter β to minimize the square of error, the equation is set to zero.

$$\partial(SSE)/\partial\beta=0 \quad (46)$$

Therefore, the column vector β can be calculated by.

$$\beta=(X^TX)^{-1}X^TY \quad (47)$$

The column vector β contains model system parameters of the tricycle vehicle in the form of a polynomial equation.

F. Improved Suspension System with Frequency Response Analysis and Damping Ratio

From FFT analysis, Peaks in the FFT plot indicate frequencies where there is a significant amount of power in the signal, which could correspond to natural frequencies or dominant oscillation modes in a system. In general, the first peak corresponds to the natural frequency of the sprung mass, and the second significant peak corresponds to the unsprung mass. However, the ISO 2631-1 standard highlights that the human body is most sensitive in the range of 4 to 8 Hz for vertical vibration. Vibrations in this range can cause discomfort, fatigue, or motion sickness as they resonate with the human body's internal organs. To reduce amplitude in the 4 to 8 Hz range, frequency response analysis, or Bode plot, is utilized to attenuate vibrations within this frequency band. This approach is known as a band-stop filter, which effectively rejects frequencies between 4 and 8 Hz while permitting frequencies outside this range to pass through. The mathematical formulation for a standard band-stop filter is expressed as

$$H(s)=s^2+\omega_0^2/s^2+\omega_c s+\omega_0^2 \quad (48)$$

Where ω_0 represents the central frequency of rejection and ω_c denotes the width of the rejected bandwidth. The Bode plot of the band-stop filter is depicted in Fig. 8. To attenuate vibrations in the 4 to 8 Hz range, the suspension parameters can be adjusted to mitigate resonance within the critical frequency range, which is associated with the characteristic equation of the transfer function H(s) G(s) [16].

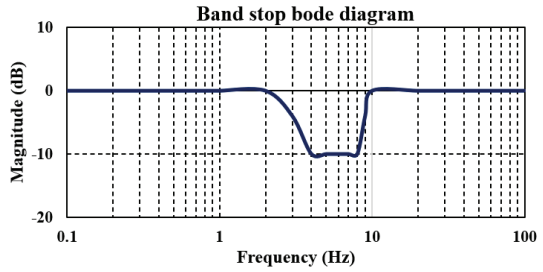

Fig. 8. The Bode plot of the band-stop filter, implemented to attenuate vibrations within the 4 to 8 Hz frequency range, is designed in compliance with the ISO 2631-1 standards.

Another criterion for riding comfort is to minimize the root mean square acceleration to below 0.315 m/s^2 or between 0.315 and 0.63 m/s^2. These vibration levels are categorized as comfortable and slightly uncomfortable, respectively. A damping ratio (ξ) of 0.3 is considered optimal for ride comfort in a vehicle suspension system, according to the ISO 2631-1 standard. At this damping ratio, the vehicle suspension system ensures that oscillations decay quickly after disturbances like bumps, potholes, or uneven road surfaces. If the damping ratio is too low, the suspension system is categorized as an underdamped system. In this case, the system will oscillate at the natural frequency, making the ride uncomfortable. If the damp ratio is too high, the suspension system is categorized as an overdamped system. In this case, the system will lead to a sluggish response, reduced ability to absorb shocks, and poor road-holding capability. The stiffness of a leaf spring can be adjusted to suit various requirements, such as riding comfort and durability. A common and straightforward method to decrease spring stiffness is to remove individual leaves from the pack, reduce the thickness of the leaves, or minimize the clamping force and friction between the leaves. Reducing the clamping or friction allows for more independent movement, which effectively reduces stiffness. The benefit of reducing spring stiffness is improved ride comfort performance. The damping coefficient of a damper, also known as a shock absorber, determines how effectively it dissipates energy and controls oscillations in a vehicle suspension system. Adjusting the damping coefficient can help achieve a balance between ride comforts and handling performance. Modifying the damping coefficient involves changing the fluid viscosity, orifice size, valve design, or gas pressure. The choice of damping coefficient depends on the specific requirements for ride comfort, stability, and handling. Reducing the damping coefficient provides a smoother ride and allows greater compliance over rough surfaces.

IV. Research Results

As for the experimental method, the researcher experimented using a system of mathematical equations to obtain the results of the experiment. The researcher divided the experimental method into three steps as follows:

A. Mathematical Calculation

After obtaining the equations of motion of the mathematical model, we then substitute the values of the variables in the equation to obtain the results of the variables whose values are not yet known. The calculation will have the following results.

$$\begin{bmatrix} -350\omega^2+479.92+509.6 & -(479.92+509.6)(0.64) \\ (-479.92+509.6)(0.64) & -140.07\omega^2+(479.92+509.6)(0.64^2) \end{bmatrix}$$

$$\begin{bmatrix} -350\omega^2+989.52 & 18.9952 \\ 18.9952 & -140.07\omega^2+405.44 \end{bmatrix}=0 \quad (49)$$

When calculating using the matrix method, the following calculation results will be obtained.

$$-350\omega^2(-140.07\omega^2+405.44)+989.52 \quad (50)$$
$$(140.07\omega^2+405.44)+ (18.9952\times18.9952)=0$$

$$49024.5\omega^4-280506\omega^2+400830=0 \quad (51)$$

By the method of finding the value of the matrix equation after substituting the values and $\Theta \neq 0$, the equation can be found using the Determinant method. This method is a function that gives the result as a scalar quantity. Which depends on the value of n in the n×n dimension of the square matrix. From the Determinant method, the equation will be obtained ω^4 and ω^2 in the form of an equation with the values of and in the equation. Arrange the form ω^2 of the equation so that, in the form ω^2 of an equation, both the equation and, when reformatting it to stay in the equation, the entire equation must then be assigned the variable $\lambda=\omega^2$ to the equation, and the roots of the equation that has been specified can be found. Obtained by using the Quadratic Formula equation. The variable values from all of the equations are $\lambda=\omega^2$, a = 49,024.5, b = -280,506, c = 400,830.

The calculation will have the following results is ω_1=1.7184 rad/s and ω_2=1.66394 rad/s. After using the Quadratic Formula equation, the natural frequencies will be obtained from the equations, all 2 natural frequencies, all of which will be in the value of and ω^2 the values that will not be negative and when obtained Once the value has been extracted, take that value and take the square root to get the angular velocity value, where the value of is the first natural frequency of the system and It is the second natural frequency of the system. After knowing the values of ω_1 and

ω_2, find the values of $X^{(1)}$ and $\theta^{(1)}$ by substituting ω_1 into the equation, and find the values of $X^{(2)}$ and $\theta^{(2)}$ by substituting ω_2 into the equation as well. When calculating using the matrix method, the following calculation results will be obtained.

(1)
$$-43.994X^{(1)}+18.9952\theta^{(1)}=0$$
$$18.9952\theta^{(1)}=43.994X^{(1)}$$

(2)
$$18.9952X^{(1)}-8.1725\theta^{(1)}=0$$
$$18.9952X^{(1)}=8.1725\theta^{(1)}$$

Find $X^{(2)}$, $\theta^{(2)}$ by plugging the result of y into the equation

$$\begin{bmatrix}20.4763 & 18.9952\\ 18.9952 & 17.6473\end{bmatrix}\begin{Bmatrix}X^{(2)}\\ \theta^{(2)}\end{Bmatrix}=\begin{Bmatrix}0\\ 0\end{Bmatrix} \quad (52)$$

When calculating using the matrix method, the following calculation results will be obtained.

(1)
$$20.4763X^{(2)}+18.9952\theta^{(2)}=0$$
$$18.9952\theta^{(2)}=20.4763X^{(2)}$$

(2)
$$18.9952X^{(2)}+17.6473\theta^{(2)}=0$$
$$17.6473\theta^{(2)}=18.9952X^{(2)}$$

When the results of the variable values are obtained, determine the ratio of the maximum amplitudes of r_1 and r_2 as follows

Find r_1 by plugging the result of y into the equation

(1)
$$r1=\theta^{(1)}/X^{(1)}=18.9952/8.1725=2.316$$

(2)
$$r1=\theta^{(1)}/X^{(1)}=43.994/18.9952=2.316$$

Find r_2 by plugging the result of y into the equation

(1)
$$r_2=\theta^{(2)}/X^{(2)}=-20.4763/18.9952=-1.078$$

(2)
$$r_2=\theta^{(2)}/X^{(2)}=-18.9952/17.6475=-1.078$$

Therefore, in order to substitute the equation to find a vibration diagram of the suspension system, it must occur at a certain time. The calculation will have the following results.

$$\vec{X}^{(1)}=\begin{Bmatrix}1\\ 2.316\end{Bmatrix}X^{(1)} \quad (53)$$

$$\vec{X}^{(2)}=\begin{Bmatrix}1\\ -1.078\end{Bmatrix}X^{(2)} \quad (54)$$

Therefore, in order to substitute the equation to find a vibration diagram of the suspension system, it must occur at a certain time. The calculation will have the following results.

[First Mode]
$$\vec{X}^{(1)}(t)=\begin{Bmatrix}X^{(1)}(t)\\ \theta^{(1)}(t)\end{Bmatrix}=\begin{Bmatrix}1\\ r_1\end{Bmatrix}X^{(1)}\cos(\omega_1 t+\emptyset_1)$$

[Second Mode]
$$\vec{X}^{(2)}(t)=\begin{Bmatrix}X^{(2)}(t)\\ \theta^{(2)}(t)\end{Bmatrix}=\begin{Bmatrix}1\\ r_2\end{Bmatrix}X^{(2)}\cos(\omega_2 t+\emptyset_2)$$

Then, solve the dynamical equation of motion (EOM) to be used in the Modal equation solving process to find the values of $X_1^{(1)}$ and $X_1^{(2)}$.

$$m\ddot{x}(t)+k_1x(t)-k_1l_1\theta(t)+k_2x(t)+k_2l_2(t)=0 \quad (55)$$

$$J_0\ddot{\theta}(t)-k_1l_1x(t)+k_1l_1^2\theta(t)+k_2l_2x(t)+k_2l_2^2\theta(t)=0 \quad (56)$$

Taking both equations and organizing them into the form of a matrix equation will be as follows:

$$\begin{bmatrix}m & 0\\ 0 & J_0\end{bmatrix}\begin{Bmatrix}\ddot{x}(t)\\ \ddot{\theta}(t)\end{Bmatrix}+\begin{bmatrix}k_1+k_2 & -k_1l_1+k_2l_2\\ -k_1l_1+k_2l_2 & k_1l_1^2+k_2l_2^2\end{bmatrix}=0 \quad (57)$$

Find the values $X_1^{(1)}$ and $X_1^{(2)}$ using the Modal method, using symbols to represent each value obtained with the symbols mentioned in (57).

The first step is to find the value of $X_1^{(1)}$ from $\vec{X}^{(i)^t}[M]\vec{X}^{(i)}=1$

$$i=1;\ \vec{X}^{(1)^t}[M]\vec{X}^{(1)}=1 \quad (58)$$

$$(X_1^{(1)})^2\{1 \quad 2.316\}\begin{bmatrix}350 & 0\\ 0 & 140.07\end{bmatrix}\begin{Bmatrix}1\\ 2.316\end{Bmatrix}=1 \quad (59)$$

$$(X_1^{(1)})^2[350 \quad 324.402]\begin{bmatrix}1\\ 2.316\end{bmatrix}=1 \quad (60)$$

$$X_1^{(1)}=1/33.186 \quad (61)$$

Therefore, then

$$\vec{X}^{(1)}=\begin{Bmatrix}1/33.186\\ 2/33.186\end{Bmatrix} \quad (62)$$

The second step is to find the value of $X_1^{(2)}$ from $\vec{X}^{(i)^t}[M]\vec{X}^{(i)}=1$

$$i=1;\ \vec{X}^{(2)^t}[M]\vec{X}^{(2)}=1 \quad (63)$$

$$(X_1^{(2)})^2\{1 \quad -1.078\}\begin{bmatrix}350 & 0\\ 0 & 140.07\end{bmatrix}\begin{Bmatrix}1\\ -1.078\end{Bmatrix}=1 \quad (64)$$

$$(X_1^{(2)})^2[350 \quad -150.99]\begin{bmatrix}1\\ -1.078\end{bmatrix}=1 \quad (65)$$

$$X_1^{(2)}=1/22.644 \quad (66)$$

Therefore, then

$$\vec{X}^{(2)}=\begin{Bmatrix}1/22.644\\ -1.078/33.186\end{Bmatrix} \quad (67)$$

In the final step, the natural frequency (Natural Frequency) or values 1 and 2 have been obtained by solving the equations mentioned above, including the values 3 and 4 from calculations through the Modal principle from Mode Shape. Vector, therefore, can be used to find the value of the Modal Matrix. When substituting the values in the equation, we will get the following:

$$[X]=\begin{bmatrix}1/33.186 & 1/22.644\\ 2/33.186 & -1.078/22.644\end{bmatrix} \quad (68)$$

$$[X]=\begin{bmatrix} 1/33.186 & 2/33.186 \\ 1/22.644 & -1.078/22.644 \end{bmatrix} \quad (69)$$

When the value [X] is obtained at a certain time, it must find the coordinates q by assigning it 180°=πrad. The calculation will have the following results.

$$\vec{q}(0)=\begin{Bmatrix} q_1(0) \\ q_2(0 \end{Bmatrix} \quad (70)$$

$$\vec{q}(0)=\begin{bmatrix} 1/33.186 & 2/33.186 \\ 1/22.644 & -1.078/22.644 \end{bmatrix}\begin{bmatrix} 350 & 0 \\ 0 & 140.07 \end{bmatrix}\begin{bmatrix} 0 \\ 0.2617 \end{bmatrix} \quad (71)$$

$$\begin{Bmatrix} q_1(0) \\ q_2(0) \end{Bmatrix}=\begin{bmatrix} 2.2091 \\ -1.7447 \end{bmatrix} \quad (72)$$

Use the solution equation of the method to find coordinates when i=1 and i=2. Use the solution equation of the method to find coordinates when i=1

$$q_i(t) = q_i(0)\cos \omega_i t+(q_i(0)/\omega_i)\sin \omega_i t \quad (73)$$

$$q_1(t) = 2.2091 \cos(1.7184)t \quad (74)$$

Use the solution equation of the method to find coordinates when i=2

$$q_i(t) = q_i(0) \cos \omega_i t+(q_i(0)/\omega_i) \sin \omega_i t \quad (75)$$

$$q_2(t) = -1.7447 \cos(1.66394)t \quad (76)$$

When the value q is obtained, it will be put into the equation to find the value $\vec{X}(t)$ by specifying the equation for finding the value. The calculation will have the following results.

$$\vec{X}(t)=\begin{bmatrix} 1/33.186 & 2/33.186 \\ 1/22.644 & -1.078/22.644 \end{bmatrix}\begin{Bmatrix} 2.2091\cos(1.7184)t \\ -1.7447\cos(1.66394)t \end{Bmatrix} \quad (77)$$

$$\vec{X}(t)=\begin{Bmatrix} 0.6657\cos 1.7184t-0.077\cos 1.66394t \\ 0.1331\cos 1.7184t+0.083\cos 1.66394t \end{Bmatrix} \quad (78)$$

B. Analysis of Results by Using Computer Programs and Comparison of Analysis Results with Comfort Standard Values

In this test, this measuring device will be assembled at various points on the tricycle. The points used in the assembly for testing are the Passenger seat and the Tricycle shaft, which will be located at the back of the tricycle. Since the researcher will only measure the vibration values for passengers.

In this section, numerous experimental results will be shown. The first experimental result is the data sets of system parameters, such as k_s is the spring constant of the suspension spring k_t is spring constant of the tire, C_s is damping coefficient of the suspension damper, in numerous conditions from the testing machine, and ξs , ξu are the damping ratios of the sprung mass and the unsprung mass, respectively. The system parameters are shown in Table II.

TABLE II
THE SYSTEM PARAMETERS OF THE TRICYCLE IN NUMEROUS CONDITIONS

Suspension Condition	System Parameters						
	k_s	k_t	C_s	m_s	m_u	ξ_s	ξ_u
Unit	N/m	N/m	$N\text{-}s/$	kg	kg	-	-
Soft	450	2710	485	350	35	0.61	0.78
Normal	510	3075	520	350	35	0.62	0.79
Hard	560	3370	614	350	35	0.69	0.89

The design and evaluation of the tricycle's body acceleration under three suspension settings—normal, hard, and soft—are illustrated in Fig. 9. Among these, the soft suspension configuration exhibits the highest variability in body acceleration. The maximum acceleration recorded under the soft suspension condition is 2.25 m/s² in the downward direction. In comparison, the maximum accelerations for the normal and hard suspension settings are 1.12 m/s² and 2.13 m/s², respectively, also in the downward direction. The Root Mean Square (RMS) values of body acceleration range from 0.985 m/s² to 1.085 m/s² across the configurations. According to ISO 2631-1, these RMS acceleration levels fall within the classification of fairly uncomfortable. Fig. 10 presents the Power Spectral Density (PSD) for each suspension condition, which represents the distribution of vibration power over frequency, computed via the Fast Fourier Transform (FFT). The primary peaks in the PSD indicate the system's natural frequencies. The first peak typically corresponds to the natural frequency of the sprung mass (vehicle body), while the second peak represents the natural frequency of the unsprung mass (wheel assembly). The observed trend shows that the natural frequency increases as the suspension stiffness is increased from soft to hard. Specifically, the natural frequency of the vehicle body ranges from 1.058 Hz to 1.181 Hz, while the natural frequency of the wheel mass varies from 9.428 Hz to 10.517 Hz, depending on the suspension setting. To attenuate vibrations within the frequency range of 4 to 8 Hz—as identified by ISO 2631-1 as critical for human comfort—a modified suspension system was designed. This design involves adjusting the damping coefficient and spring stiffness, which are directly related to the characteristic equation of the combined transfer function $H(s) \cdot G(s)$, where $H(s)$ is a band-stop filter designed to reject vibrations in the 4 to 8 Hz range, and $G(s)$ is the transfer function of the vehicle suspension system. The modified suspension parameters include a spring constant of k_s = 485 N/m, a tire stiffness of k_t = 2,214 N/m, and a damping coefficient of C_s = 253 Ns/m, achieving a damping ratio of 0.3 for improved ride comfort. Fig. 11 compares the PSD results of the normal and modified suspension systems. The modified configuration demonstrates

a significant reduction in spectral amplitudes within the 4 to 8 Hz range, indicating effective vibration rejection. The RMS acceleration for the modified suspension system is reduced to 0.537 m/s², which, according to ISO 2631-1, corresponds to a comfort level categorized as slightly uncomfortable. This marks an improvement in ride quality from the previously classified fairly uncomfortable level. Fig. 12 illustrates the time-domain acceleration response of the tricycle body under normal and modified suspension conditions. The maximum body acceleration under the normal suspension is 1.12 m/s² in the downward direction, whereas the modified suspension reduces this peak to 0.582 m/s². These findings confirm that the modified suspension configuration enhances ride comfort by mitigating both the amplitude and variability of vibrations experienced by the vehicle body.

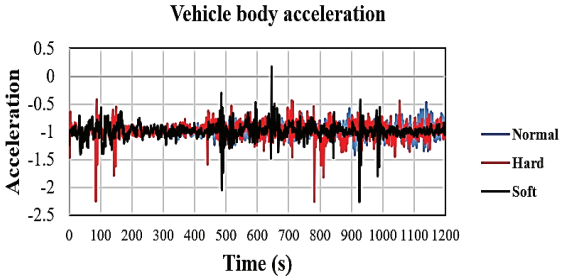

Fig. 9. Vehicle body acceleration in normal, hard, and soft conditions of the suspension system

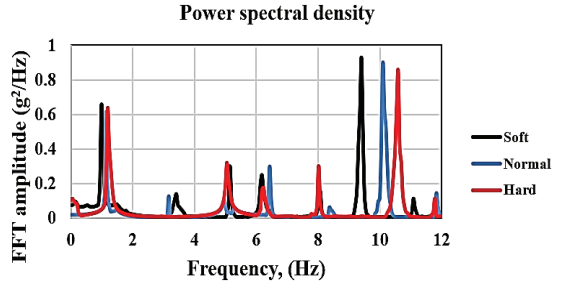

Fig. 10. Power spectral density in normal, hard, and soft conditions of the suspension system

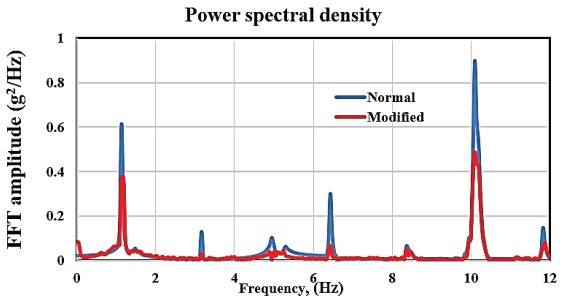

Fig. 11. Power spectral density in normal and modified conditions of the suspension system

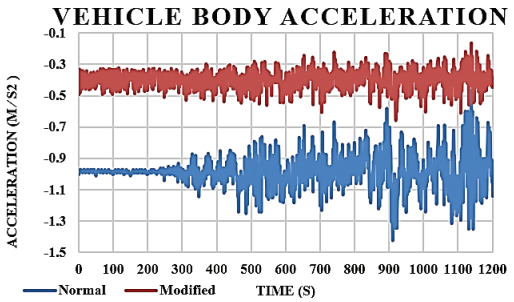

Fig. 12. The tricycle vehicle body acceleration when the suspension systems have been adjusted to normal and modified conditions

V. Discussion

The experimental results demonstrate the significant influence of suspension settings on ride comfort and the dynamic response of a tricycle structure. Among the tested conditions, soft, normal, and hard suspension, the soft suspension setting resulted in the highest variation in vehicle body acceleration, with a maximum downward acceleration of 2.25 m/s². This indicates that the damping in this condition is insufficient, allowing a considerable amount of road-induced vibration to be transmitted into the vehicle structure. In contrast, the normal and hard suspension setups provided greater stability, with reduced maximum accelerations of 1.12 m/s² and 2.13 m/s², respectively. However, while the hard suspension reduced overall body movement, it increased discomfort due to higher-frequency vibrations. The Root Mean Square (RMS) acceleration values ranged from 0.985 to 1.085 m/s², which, according to ISO 2631-1, is categorized as Fairly Uncomfortable. This suggests that none of the tested suspension configurations provided truly satisfactory ride comfort. The analysis of the Power Spectral Density (PSD) supports these findings, revealing spectral peaks corresponding to the system's natural frequencies, which vary depending on the suspension condition. The vehicle body's natural frequency increased from 1.058 Hz (soft) to 1.181 Hz (hard), while the wheel mass frequency rose from 9.428 Hz to 10.517 Hz. These results confirm that suspension stiffness has a direct effect on vibration behavior. To improve ride comfort, a modified suspension system was developed by adjusting the damping coefficient (Cs = 253 N·s/m) and spring constants (k_s = 485 N/m, k_t = 2,214 N/m). The goal was to reduce vibrations in the 4-8 Hz range—a frequency range to which the human body is particularly sensitive. This was achieved using a band-stop transfer function H(s) in combination with the vehicle suspension transfer function G(s) to reject vibrations in this range. After modification, the RMS acceleration

was reduced to 0.537 m/s², which falls under the category of Slightly Uncomfortable per ISO 2631-1. This indicates a clear improvement in ride comfort. The maximum downward acceleration of the vehicle body decreased from 1.12 m/s² (normal suspension) to only 0.582 m/s² (modified suspension). From these results, it can be concluded that targeted tuning of the suspension system, guided by vibration analysis and ISO 2631-1 standards, can effectively enhance ride comfort—both by reducing overall acceleration levels and minimizing vibration energy within sensitive frequency bands. For future studies, the use of adaptive or semi-active suspension systems may be considered to better accommodate various road conditions and further improve comfort.

VI. Conclusions

This study confirms that suspension tuning plays a critical role in enhancing ride comfort for tricycle vehicles. Among the tested configurations, the modified suspension system designed to attenuate vibrations within the sensitive frequency range of 4 to 8 Hz provided the most favorable results. It significantly reduced both peak acceleration and Root Mean Square (RMS) values, improving the ride comfort classification from fairly uncomfortable to slightly uncomfortable based on ISO 2631-1 standards. These findings underscore the importance of systematic suspension design based on vibration analysis and standard-based performance criteria. The proposed approach demonstrates that targeted adjustment of damping and stiffness parameters can effectively mitigate uncomfortable vibrations. Furthermore, the combined use of mathematical modeling, simulation, and experimental validation offers a robust framework for optimizing suspension systems. This methodology may be extended to other vehicle types, and future research could explore the implementation of adaptive or semi-active suspension systems to enhance performance under varying road conditions.

References

[1] Department of Land Transport, "Annual report 2021," *Dept. Land Transp.*, 2022. [Online]. Available: https://rapi.mot.go.th/uploads/2564_e0ce69451d.pdf [Accessed: Dec. 18, 2024].

[2] S. Isarnawe, S. Chattharupracha, and S. Khetprathum, "Design and development of suspension parts for in-wheel TMAC Formula," Ph.D. dissertation, Naresuan Univ., Phitsanulok, Thailand, 2017.

[3] S. S. Rao, *Mechanical Vibrations*, 5th ed. Upper Saddle River, NJ, USA: Pearson, 2010, pp. 129-130.

[4] S. S. Rao, *Mechanical Vibrations*, 5th ed. Upper Saddle River, NJ, USA: Pearson, 2010, p. 159.

[5] R. Darus and Y. M. Sam, "Modeling and control active suspension system for a full car model," in *Proc. 5th Int. Colloq. Signal Process. Appl. (CSPA)*, 2009, pp. 13-18.

[6] K. Jaisaard and W. Santipach, "A comparative study of ride comfort between EMU-A1 and EMU-B1 trains of BTS on Sukhumvit line from N8 to E14 stations," Ph.D. dissertation, Kasetsart Univ., Bangkok, Thailand, 2021.

[7] Arduino LLC, "Arduino," *Arduino off Website*, 2015. [Online]. Available: https://www.arduino.cc/ [Accessed: Dec. 18, 2024].

[8] A. Guo, "Vibration sensor design research," *Sens. Transducers*, vol. 169, no. 4, pp. 228-232, Apr. 2014.

[9] U. T. Ceyhanli and M. Bozca, "Experimental and numerical analysis of the static strength and fatigue life reliability of parabolic leaf springs in heavy commercial trucks," *Mech. Eng.*, vol. 12, no. 7, pp. 1-17, Jul. 2020.

[10] S. S. Rao, *Mechanical Vibrations*, 5th ed. Upper Saddle River, NJ, USA: Pearson, 2010, pp. 472-480.

[11] A. Shirahatti, P. S. S. Prasad, P. Panzade, and M. M. Kulkarni, "Optimal design of passenger car suspension for ride and road holding," *J. Braz. Soc. Mech. Sci. Eng.*, vol. 30, pp. 66-76, 2008.

[12] S. S. Rao, *Mechanical Vibrations*, 5th ed. Upper Saddle River, NJ, USA: Pearson, 2010, p. 502.

[13] S. S. Rao, *Mechanical Vibrations*, 5th ed. Upper Saddle River, NJ, USA: Pearson, 2010, pp. 654-698.

[14] D. Hanafi, "PID controller design for semi-active car suspension based on model from intelligent system identification," in *Proc. 2nd Int. Conf. Comput. Eng. Appl. (ICCEA)*, 2010, pp. 60-63.

[15] A. Anandan and A. Kandavel, "Investigation and performance comparison of ride comfort on the created human–vehicle–road integrated model adopting genetic algorithm optimized proportional–integral–derivative control technique," *Inst. Mech. Eng., Part K: J. Multi-body Dyn.*, vol. 234, no. 2, pp. 288-305, Feb. 2020.

[16] V. Popovic, D. Jankovic, and B. Vasic, "Design and simulation of active suspension system by using MATLAB," *SAE Tech. Paper*, no. 2000-05-0180, 2000. [Online]. Available: https://doi.org/10.4271/2000-05-0180 [Accessed: Jan. 10, 2025].

[17] S. Chow, P. Eisen, H. Johnson, and P. C. van Oorschot, "White-box cryptography and an AES implementation," in *Proc. 9th Annu. Int. Workshop Sel. Areas Cryptogr. (SAC)*, 2002, pp. 250-270.

[18] J. Lu, H. Sibai, and E. Fabry, "Adversarial examples that fool detectors," *arXiv*, 2017. [Online]. Available: https://arxiv.org/abs/1712.02494 [Accessed: Apr. 14, 2024].

[19] S. Nidhra and J. Dondeti, "Black box and white box testing techniques—a literature review," *Int. J. Eng. Sci. Adv. Technol. (IJESA)*, vol. 2, no. 2, pp. 29-50, Jun. 2012.

[20] W. Hui, "Physical adversarial attack meets computer vision: A decade survey," *arXiv*, 2022. [Online]. Available: https://arxiv.org/abs/2209.15179 [Accessed: Jan. 20, 2024].

[21] C. Sitawarin, A. N. Bhagoji, A. Mosenia, and P. Mettal, "Rogue signs: Deceiving traffic sign recognition with malicious ads and logos," *arXiv*, 2018. [Online]. Available: https://arxiv.org/abs/1801.02780 [Accessed: Apr. 15, 2024].

[22] I. Evtimov et al., "Robust physical-world attacks on machine learning models," *arXiv*, 2017. [Online]. Available: https://arxiv.org/abs/1707.08945 [Accessed: Jan. 20, 2024].

[23] Z. Zhang and M. Sabuncu, "Generalized cross entropy loss for training deep neural networks with noisy labels," *arXiv*, 2018. [Online]. Available: https://arxiv.org/abs/1805.07836 [Accessed: Jan. 20, 2024].

Chaiyawoot Narintharangkul graduated with a degree in Automotive Manufacturing Engineering from Panyapiwat Institute of Management, Thailand, in March 2020, and is currently pursuing a master's degree in the Faculty of Engineering and Technology. Used to work as an Inspection Engineer trainee at Keisokukensa Company in 2020. Currently, a job as a Senior Officer in the Engineering and Technology Faculty at Panyapiwat Institute of Management, Nonthaburi, Thailand.

Poom Jatunitanon received a Doctor of Engineering in Mechanical Engineering from Kasetsart University, Thailand, in 2017. Used to be a professor in automotive manufacturing engineering, from 2019 to 2025 at the Faculty of Engineering and Technology at Panyapiwat Institute of Management, Thailand, and current job as Head of automotive manufacturing engineering at the Faculty of Engineering and Technology at Panyapiwat Institute of Management, Nonthaburi, Thailand.